Helix–Coil Transitions in a Simple Polypeptide Model

J. A. McCAMMON and S. H. NORTHRUP, *Department of Chemistry, University of Houston, Houston, Texas 77004;* and M. KARPLUS and R. M. LEVY, *Department of Chemistry, Harvard University, Cambridge, Massachusetts 02138*

Synopsis

A simplified model of a polypeptide chain is described. Each residue is represented by a single interaction center. The energy of the chain and the force acting on each residue are given as a function of the residue coordinates. Terms to approximate the effect of solvent and the stabilization energy of helix formation are included. The model is used to study equilibrium and dynamical aspects of the helix–coil transition. The equilibrium properties examined include helix–coil equilibrium constants and their dependence on chain position. Dynamical properties are examined by a stochastic simulation of the Brownian motion of the chain in its solvent surroundings. Correlations in the motions of the residues are found to have an important influence on the helix–coil transition rates.

INTRODUCTION

The helix–coil transition in polypeptides has been the subject of many experimental and theoretical studies.[1–3] Much of the interest is due to the probable role of such transitions in nucleating the folding of globular proteins[4–8] and in other biochemical processes such as certain hormone–receptor interactions.[9,10] In spite of the considerable work in the area, no detailed theoretical analysis of the dynamics of the helix–coil transition is available. An essential difficulty in making such an analysis is that the time scale of the helix–coil transition is on the order of 10^{-9}–10^{-6} sec, while dynamical-simulation methods for an all-atom model of the polypeptide chain are limited to the range of 10^{-12}–10^{-9} sec.[11] To overcome this problem we utilize a simplified model for the polypeptide chain that makes it possible to treat the time range appropriate for the helix–coil transition. The approach used is an extension to polypeptide chains of methods commonly employed in the dynamics of polymers.[12–17] In the present paper, a model for the polypeptide chain in aqueous solution is described and applied in preliminary simulation studies of the helix–coil transition. The simplified character of the model permits rapid calculation of the polypeptide energy and the forces acting on individual residues, including solvent effects. This feature allows extensive configuration sampling, which is required in studies of the equilibrium and dynamical properties of interacting polypeptides, as well as of isolated chains.

Biopolymers, Vol. 19, 2033–2045 (1980)

0006-3525/80/0019-2033$01.30

In the simplified model, each residue is represented by a soft sphere with a volume similar to that of the corresponding amino acid. A recent analysis of the x-ray structure of myoglobin by Richmond and Richards[18] suggests that this kind of model can provide an adequate description of the residue packing in α-helices. Conformational mobility of the chain is permitted by torsional motions around virtual bonds which link the residues in a linear sequence. The energy function for the chain represents a balance between interactions which tend to stabilize the helical conformation and interactions which tend to stabilize coil conformations. While such a model cannot accurately represent the detailed atomic interactions (such as side-chain hydrogen bonds), it can provide an approximate description of the overall structure and flexibility of polypeptides with less specific side-chain interactions (e.g., steric and hydrophobic interactions).

The motions of the simplified chain in water are simulated by a stochastic dynamics method.[13–17,31] The resulting trajectories represent the slow, diffusional fluctuations in the overall conformation of the chain. On the time scale of these fluctuations, localized motions such as side-chain internal rotations are rapidly averaged so that the simplified structural model is appropriate. With this method, the overall motions of a chain can be simulated for periods of several hundred nanoseconds. Thus, the method is useful for studies of processes which occur on the nanosecond time scale and in which side-chain interactions are dominated by simple packing effects. It is expected that the choice of the model and its energy parameters, which yield satisfactory values for the helix–coil equilibrium properties, are appropriate for treating the helix–coil dynamics. The method would not be useful for simulating the folding of an entire protein, for example, since this process occurs on a much longer time scale and will typically involve detailed atomic interactions in the formation of tertiary structure.[4,5]

POLYPEPTIDE MODEL

The model described here is based on the virtual-bond formulation introduced by Flory,[12] developed for polypeptide chains by Levitt and Warshel,[19,20] and simplified by Levitt for molecular-dynamics simulations.[21] Each amino acid residue is represented by a single interaction center, R_i (Fig. 1). These centers are linked by virtual bonds and bond angles with harmonic restoring potentials. An intrinsic torsional potential is associated with each virtual dihedral angle to represent the average sum of nonbonded interactions between the atoms of near-neighbor residues. (The virtual dihedral angle Φ_i is defined in terms of the centers of residues $i, i+1, i+2$, and $i+3$; $\Phi_i = 0$ for the eclipsed conformation.) Interactions between residues separated by three or more virtual bonds are given by central force potentials which represent excluded-volume and net attractive effects in aqueous surroundings. Finally, additional torsional potentials are used to represent special interactions (e.g., backbone hydrogen bonds)

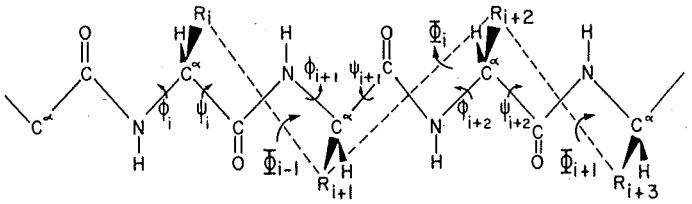

Fig. 1. The geometry of the simplified polypeptide model, compared with that of the atomic model. The dashed lines are virtual bonds connecting the interaction centers R_i.

which stabilize helical conformations. The sum of all these potential terms constitutes the simplified energy function for the polypeptide.

In representing the large-scale conformational changes of the polypeptide, only the torsional motions of the simplified chain are significant; this point is considered in the Discussion. The bond and bond-angle potentials could in fact be replaced by rigid constraints[19,20]; flexible potentials are used here to simplify the force calculations in Cartesian coordinates and to avoid certain modifications of the energy function which would be required if constraints were used.[22]

For the initial studies described here, the geometric and energy parameters of the simplified model were chosen to correspond to polyvaline; generalization to other homopolymers or to heteropolymers is straightforward. Details are given in the following two subsections, but the essential features of the resulting model may be briefly summarized as follows. Residues in a coil region experience a relatively soft torsional potential; the presence of the excluded-volume terms prevents overlap of nonbonded residues. A residue in the helix–coil interface is stabilized in the helical conformation by a narrow potential well with a depth of about 2 kcal/mol, and in the coil conformation by a broad potential well with a depth of about 1 kcal/mol. Residues in the interior of the helix are confined to the helical conformation by a narrow potential well with a depth of about 6 kcal/mol.

Geometry

The equilibrium bond lengths and bond angles of the simplified chain, as well as the characteristic dihedral-angle value for an α-helix, were calculated by reference to a detailed atomic model constructed with standard α-helix geometry.[23] The interaction centers of the simplified chain were placed at the C^β positions in the detailed structure, i.e., close to the valine centroids defined by Levitt.[21] From this arrangement of interaction centers, the desired internal coordinate values were found to be $b_0 = 5.14$ Å, $\Theta_0 = 87.2°$, and $\Phi_\alpha = 38.3°$ for the equilibrium bond length, equilibrium bond angle, and α-helix dihedral angle, respectively. From Fig. 2 of Ref. 20, the width of the α-helix region is about 30°; thus, $25° < \Phi < 55°$ was taken to define the α-helical region for the simplified chain.

Energy Function

The energy function described here is chosen to approximate the potential of mean force which corresponds to a thermal average over polypeptide degrees of freedom that are omitted in the simplified model and over solvent molecule degrees of freedom.[24] This point is considered further in the Discussion. The function is a sum of six kinds of interactions:

$$E = E_{\text{bond}} + E_{\Theta} + E_{\Phi} + E_{\text{sol}} + E_{\text{ev}} + E_{\alpha} \tag{1}$$

The bond and bond-angle interactions are harmonic:

$$E_{\text{bond}} = \sum k_b (b - b_0)^2 \tag{2}$$

$$E_{\Theta} = \sum k_{\Theta} (\Theta - \Theta_0)^2 \tag{3}$$

where the summations are over all the virtual bonds and virtual bond angles, respectively. The force constants are[21] $k_b = 40$ kcal mol^{-1} Å^{-2}, $k_{\Theta} = 40$ kcal mol^{-1} rad^{-2}, and $b_0 = 5.14$ Å, $\Theta_0 = 1.52$ rad $= 87.2°$.

The third term in the energy function represents near-neighbor atomic nonbonded interactions, averaged over all dihedral angles consistent with a given value of Φ in a detailed dipeptide model:

$$E_{\Phi} = \sum V(\Phi) \tag{4}$$

where the summation is over all the virtual dihedral angles and $V(\Phi)$ is the Fourier series for Ala-Ala dipeptides given by Levitt.[20]

The attractive van der Waals and solvent contribution has the *ad hoc* form given by Levitt for valine residues[20,25]:

$$E_{\text{sol}} = \sum \sigma g(r_{ij}), \qquad i > j \tag{5}$$

where r_{ij} is the distance between interaction centers i and j, $g(r)$ is a sigmoid function which varies from $g(0) = 1$ to $g(r) = 0$ for $r > 9$ Å, $\sigma = -3.0$ kcal/mol, and the sum is taken over centers separated by three or more bonds.

The excluded-volume term is given by

$$E_{\text{ev}} = \sum V_{\text{ev}}(r_{ij}), \qquad i > j \tag{6}$$

where

$$V_{\text{ev}}(r) = \begin{cases} \epsilon \left[3 \left(\dfrac{r^\circ}{r} \right)^8 - 4 \left(\dfrac{r^\circ}{r} \right)^6 + 1 \right], & r < r^\circ \\ 0, & r > r^\circ \end{cases} \tag{7}$$

and $\epsilon = 0.33$ kcal/mol, $r^\circ = 6.5$ Å, corresponding to Levitt's "whole residue" parameters for valine.[20] This contribution, which differs from Levitt's in that it is purely repulsive, is obtained from his van der Waals potential function by the repulsive-potential construction introduced by Weeks et al.[26] This substitution of a purely repulsive potential takes cognizance of

the fact that the surrounding of one valine residue by other valine residues represents a transfer from an aqueous surrounding and not from a vacuum. The change in attractive interactions upon such a transfer is already included in the solvation energy term, which is derived from the free energy of transfer of residues from aqueous to hydrophobic surroundings.[25] The present choice, which is introduced in part to prevent the excessive stability of valine "globules" in the coil portion of the chain (see Discussion), is in better accord with the hydrophobic interaction theory of Pratt and Chandler[27] and with detailed simulation studies of hydrophobic interactions[28,29] in terms of the depth of the net attractive potential well.

The helix-stabilization energy is given by

$$E_\alpha = \sum A_\Phi f(\Phi) \tag{8}$$

where the summation runs over all the virtual dihedral angles. The function $f(\Phi)$ is bell-shaped, with a maximum value of unity at $\Phi = 40°$; $f(\Phi)$ and its first derivative vanish at $\Phi = 25°$ and 55°. The detailed form of $f(\Phi)$ for $25° < \Phi < 55°$ is

$$f(\Phi) = 55.73[0.7854(\Phi - a_\pm)^2 \pm 2.0(\Phi - a_\pm)^3] \tag{9}$$

where Φ is in radians, $a_+ = 0.9599$ rad, $a_- = 0.4363$ rad; the upper signs are used if $40° < \Phi < 55°$, the lower signs if $25° < \Phi < 40°$. $f(\Phi) = 0$ if Φ is outside the α-helical range. The coefficient A_Φ for each dihedral angle depends on adjacent dihedral angles according to the following rules. (The rules are adequate for modeling growth and decay at the end of a single helical sequence, which is the only problem considered here.) If Φ_{i-1}, Φ_{i-2}, . . . , Φ_1 and Φ_{i+1} are in the α-helix range, $A_{\Phi_i} = -6.0$ kcal/mol, reflecting the difficulty of nucleating a coil sequence in the interior of an α-helix.[1] If Φ_{i-1}, Φ_{i-2}, . . . , Φ_1 are in the α-helix range but Φ_{i+1} is not, $A_{\Phi_i} = -1.4$ kcal/mol. If Φ_i is not in the helix interior or at the helix–coil interface, $A_{\Phi_i} = 0$. Thus, if Φ_i is in the range $25° < \Phi_i < 55°$, it is considered to be in the α-helix only if $\Phi_{i-1}, \ldots, \Phi_1$ are also in the helix; this reflects the difficulty of nucleating a new section of helix.[1] The value $A_\Phi = -1.4$ kcal/mol for the helix–coil interface was chosen to approximately reproduce the experimental s parameter for valine, as described in the next section.

EQUILIBRIUM PROPERTIES

Several average quantities were calculated for residues at a helix–coil interface. The first of these is the equilibrium constant s_i for transformation of a residue at the end of a section of helix from a coil state to a helix state[1]:

$$\ldots hhc_ic \ldots \rightleftarrows \ldots hhh_ic \ldots$$

$$[h_i]/[c_i] = s_i \tag{10}$$

In addition, the various components of the potential of mean force for a residue at the end of a section of helix were computed.

The calculations were performed for a 15-residue chain (12 dihedral angles) by the following method. To calculate average quantities for residue $i + 3$, the dihedral angles $\Phi_1, \Phi_2, \ldots, \Phi_{i-1}$ were held fixed at 38.3°; that is, residues $1, 2, \ldots, i + 2$ formed a section of α-helix. The angle Φ_i was varied over values $\Phi_i = 0°, 10°, \ldots, 350°$; and $\Phi_{i+1}, \ldots, \Phi_{12}$ were varied over values $\Phi = 0°, 30°, \ldots, 330°$. For each value of Φ_i, the Boltzmann factors corresponding to all values of $\Phi_{i+1}, \ldots, \Phi_{12}$ were summed:

$$P'(\Phi_i) = \sum \exp[-E(\Phi_i, \Phi_{i+1}, \ldots, \Phi_{12})/RT] \tag{11}$$

where the summation runs over the values of $\Phi_{i+1}, \ldots, \Phi_{12}$; R is the gas constant and $T = 300°$ K. $E(\Phi_i, \Phi_{i+1}, \ldots, \Phi_{12})$ includes only the torsional functions for the indicated dihedral angles and those nonbonded interactions which change upon variation of these dihedral angles. In accordance with the rules given above, the A_Φ in Eq. (8) were fixed as $A_{\Phi_i} = -1.4$ kcal/mol, $A_{\Phi_{i+1}} = \cdots = A_{\Phi_{12}} = 0$.

$P'(\Phi_i)$ is proportional to the probability of finding residue $i + 3$ in the state defined by a particular value of Φ_i, given that residues $1, \ldots, i + 2$ form an α-helix and residues $i + 4, \ldots, 15$ sample all possible coil configurations. The absolute probabilities are computed by normalization:

$$P(\Phi_i) = Z_i^{-1} P'(\Phi_i) \tag{12}$$

where Z_i is the configurational sum over the values of Φ_i:

$$Z_i = \sum P'(\Phi_i) \tag{13}$$

The equilibrium constant s_{i+3} is the probability of finding residue $i + 3$ in a helix state divided by the probability of finding it in a coil state. These equilibrium constants were estimated by computing

$$s_{i+3} = \sum P(\Phi_i) / \sum P(\Phi_i) \tag{14}$$

where the sum in the numerator runs over $\Phi_i = 30°, 40°, 50°$, and that in the denominator runs over all other values of Φ_i. This ratio is relatively insensitive to the angular sampling interval, since the numerator is dominated by the 40° term.

To obtain information concerning the kinds of interaction which make particular values of Φ_i more or less probable at the helix–coil interface, we compute the components of the potential of mean force for Φ_i. The jth component of the potential of mean force is denoted by $\langle E_j(\Phi_i) \rangle$, where E_j represents any of the terms in Eq. (1) or the sum of these terms. $\langle E_j(\Phi_i) \rangle$ is the average energy obtained by fixing residue $i + 3$ in the state defined by a particular value of Φ_i, fixing residues $1, \ldots, i + 2$ in an α-helix and allowing residues $i + 4, \ldots, 15$ to sample all coil configurations with Boltzmann weighting:

$$\langle E_j(\Phi_i) \rangle = \sum E_j(\Phi_i, \ldots, \Phi_{12}) P(\Phi_{i+1}, \ldots, \Phi_{12} | \Phi_i) \tag{15}$$

where the sum is over the values of $\Phi_{i+1}, \ldots, \Phi_{12}$. $P(\Phi_{i+1}, \ldots, \Phi_{12} | \Phi_i)$ is the probability of finding the coil configuration $\Phi_{i+1}, \ldots, \Phi_{12}$, given that

Φ_i has the indicated value and $\Phi_1 = \cdots = \Phi_{i-1} = 38.3°$. This probability is

$$P(\Phi_{i+1}, \ldots, \Phi_{12}|\Phi_i) = \frac{\exp[-E(\Phi_i, \ldots, \Phi_{12})/RT]}{P'(\Phi_i)} \tag{16}$$

where $P'(\Phi_i)$ is given by Eq. (11).

Using the methods described above, the equilibrium constants s_i and the various components of the potentials of mean force were computed for residues 15 (the terminal residue in the chain), 14, 13, 12, and 11. The resulting s_i parameters are listed in Table I. The insensitivity of the s_i parameters with respect to chain position is in accord with the usual Ising model assumptions.[1] The s_i parameters are, however, quite sensitive to the value chosen for the helix-stabilization energy coefficient A_Φ at the helix–coil interface. The value $A_\Phi = -1.4$ kcal/mol was chosen to produce approximate agreement with the experimental result for polyvaline in water at 25°C, $s = 0.95$.[30] With $A_\Phi = -1.6$ kcal/mol, one finds $s = 1.3$ for residue 12; with $A_\Phi = -1.0$ kcal/mol, one finds $s = 0.6$ for residue 12. It should also be noted that if the attractive part is left in the van der Waals potential [Eq. (6)], the polypeptide displays an overwhelming tendency to fold into a globular "coil" conformation. To obtain s parameters near unity in this case, A_Φ would have to decrease rapidly for dihedral angles farther into the chain; e.g., $A_\Phi < -10$ kcal/mol would be required for Φ_8.

The components of the potential of mean force for residue 12, $\langle E_j(\Phi_9)\rangle$, are shown as functions of Φ_9 in Fig. 2. Results for the other residues are nearly identical with those shown. Outside the range $20° < \Phi_9 < 240°$, the potential of mean force is dominated by large, repulsive excluded-volume contributions that result from close contacts between residue 12 and the helix; these contacts yield smaller, attractive contributions through E_{sol}. The small rise in the excluded-volume contribution near $\Phi_9 = 180°$ is due to packing of the coil residues against the helix; this is the structure which would predominate if the attractive part were left in the van der Waals potential.

DYNAMICAL PROPERTIES

An initial study of the dynamics of the helix–coil transitions for the 15-residue chain was carried out by simulating the internal Brownian motion of the chain in its solvent surroundings. In the simulation method

TABLE I
Helix–Coil Equilibrium Constants in a 15-Residue Chain

Residue	s
15	1.03
14	1.05
13	1.01
12	1.01
11	1.01

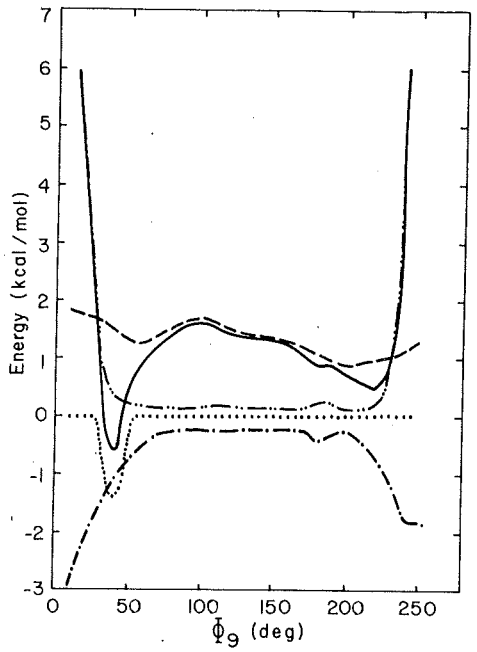

Fig. 2. Potential of mean force and its components for a residue at the helix–coil interface for E (—), E_Φ (- - -), E_{sol} (·-·-), E_{ev} (-··-), and E_α (···).

used here, each successive configuration of the chain is selected from a probability distribution which is the short-time solution of the chain-diffusion equation with the previous configuration as an initial condition.[31] Diffusional trajectories generated by this method accurately represent possible chain motions if the time step is short enough that the systematic forces derived from Eq. (1) change only slightly during each step. In addition, the momentum relaxation time of the residues must be short on the time scale of the residue displacements, since inertial effects are incompletely damped over intervals shorter than the momentum relaxation time, and these effects are not reproduced by the simulation method. Hydrodynamic interactions among the residues have been neglected in these preliminary calculations.

The diffusion constants for the residues are taken to be $D = 6.71 \times 10^{-6}$ cm^2/sec, corresponding to spheres of radius 3.25 Å in water at 25°C. Trial computations indicated that a fairly short time-step ($\Delta t = 0.03$ psec) is required for the dihedral angles in the helix–coil interface to follow the effective torsional potentials faithfully. This is a consequence of the sizable nonbonded interactions in this region. The angular momentum relaxation time for torsional motions of the residues can be shown to be comparable to or smaller than the time step given above. Using Kramers' criterion,[32] it can also be shown that frictional effects overwhelmingly dominate inertial effects when residues cross the free-energy barrier separating helix and coil states.

In this study, the chain was initially in an all-helical configuration. The first 11 residues were held fixed in space, while the last 4 residues were allowed to move. Three independent simulations were performed, each for a total length of 12 nsec. The time histories of the last three dihedral angles are shown in Figs. 3–5; Φ_9, which showed relatively little mobility, is omitted from these figures for clarity. Points are plotted at intervals of 120 psec.

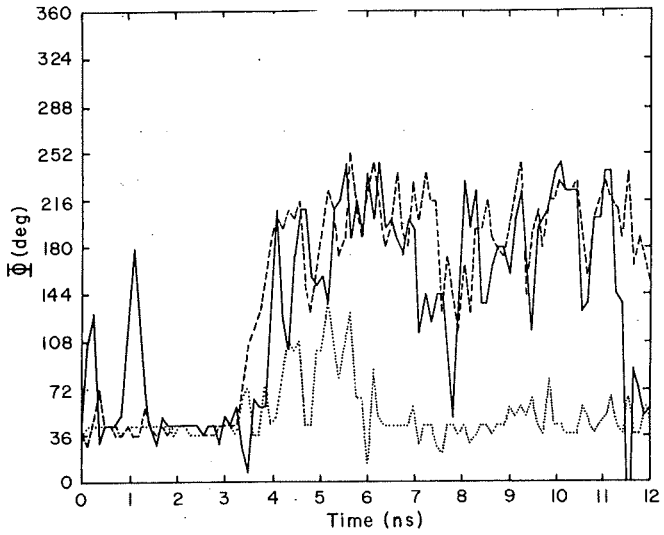

Fig. 3. Dihedral-angle histories during the first helix-unwinding simulation: Φ_{12} (—), Φ_{11} (- - -), and Φ_{10} (···).

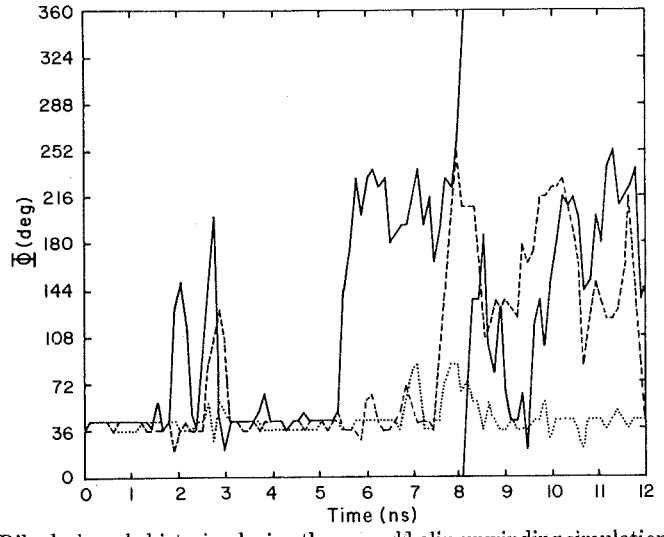

Fig. 4. Dihedral-angle histories during the second helix-unwinding simulation: Φ_{12} (—), Φ_{11} (- - -), and Φ_{10} (···).

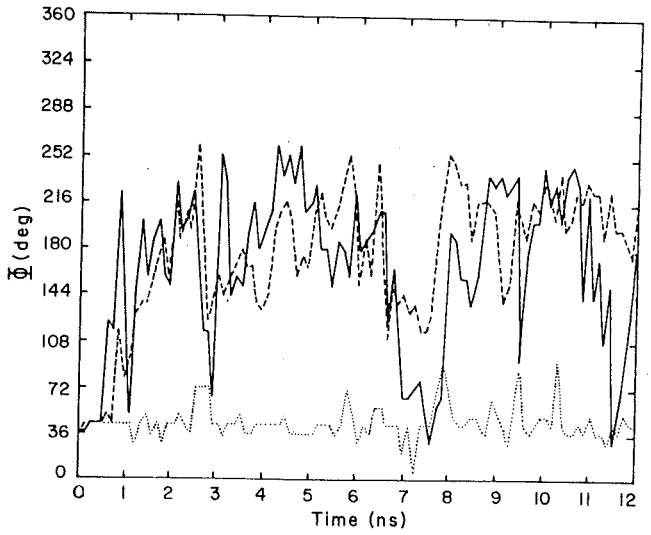

Fig. 5. Dihedral-angle histories during the third helix-unwinding simulation: Φ_{12} (—), Φ_{11} (- - -), and Φ_{10} (···).

In examining these figures, it is important to recall that helix–coil transitions occur only at the end of the single helical section; if Φ_i is in the range $25° < \Phi_i < 55°$, it is considered to be in the α-helix only if $\Phi_{i-1}, \ldots, \Phi_1$ are also in the helix. Nucleation of a second section of helix would be exceedingly rare on the time scale of these simulations.[2]

Significant unwinding of the helix occurs in each simulation. The runs are not long enough to yield equilibrium sampling of the mobile portion of the chain, however. When two or more residues leave the helix, they do so sequentially; this is not always apparent in the figures due to the 120-psec plotting interval used. After unwinding, Φ_{12} and Φ_{11} tend to remain in the range $120° < \Phi < 260°$, although Φ_{12} often drifts to smaller values and Φ_{11} returns to the helix at the end of the second simulation. The results of these simulations are further considered below.

DISCUSSION

Polypeptide Model and Equilibrium Properties

The simplified polypeptide model has only one backbone rotational degree of freedom per residue (Φ), while the detailed atomic model has two (ϕ and ψ). Examination of Fig. 1 shows that for given positions of the simplified residues R_i, R_{i+1}, R_{i+2}, the position of R_{i+3} is essentially determined by ψ_{i+1} and ϕ_{i+2} through the sum $\psi_{i+1} + \phi_{i+2}$.[12] Variations in the difference $\psi_{i+1} - \phi_{i+2}$ correspond to rotations of the plane of the amide group between residues $i + 1$ and $i + 2$; such rotations have a relatively small effect on the overall chain direction. In the simplified model, the position

of R_{i+3} is determined by Φ_i, which essentially depends only on $\psi_{i+1} + \phi_{i+2}$. Thus, the energy function used here is a potential of mean force which is averaged over amide plane orientations as well as side-chain and solvent-molecule configurations.

In the simplified model, if R_i, R_{i+1}, and R_{i+2} are part of an α-helix, R_{i+3} is added to the helix when Φ_i enters the helical region. Inspection of Fig. 1 shows that the amide plane between residues $i + 2$ and $i + 3$ must also assume the correct orientation, so that the amide NH can form a hydrogen bond with the CO of residue $i - 1$. The freezing of this amide plane results in an entropy reduction which is considered below. In the dynamical simulations, where only Φ angles are explicitly considered, it is assumed that the local reorientations of the amide planes are rapid compared to the variations in Φ, which reflect the slow changes in the overall shape of the chain.

The α-helix stabilization term in the energy function contributes up to -1.4 kcal/mol upon the addition of a residue to the helix. This term includes free-energy changes associated with the formation of a backbone hydrogen bond and the freezing of amide-plane rotational motions. While it is difficult to give precise values for these changes, calorimetric and pH titration studies of helix–coil transitions suggest that hydrogen-bond formation, with an estimated free-energy change of -1.5 kcal/mol, provides the larger contribution.[33,34] Since the typical range of variation of amide plane orientations is about 180° or less for nonhelical residues in proteins (see Fig. 2 in Ref. 20), the entropy reduction upon freezing the amide-plane orientation is less than 2 e.u. (Ref. 35); this corresponds to a free-energy increase at 25°C of less than 0.6 kcal/mol. Thus, the stabilization energy used here appears to be of a reasonable magnitude.

The potential of mean force shown in Fig. 2 exhibits a free-energy barrier of roughly 1 kcal/mol for the coil-to-helix transition; the coil state is stabilized primarily by favorable near-neighbor nonbonded interactions (as reflected in E_Φ) and, to a lesser extent, by hydrophobic interactions. Recent measurements of the temperature dependence of the helix growth rates of two different polypeptides yielded low apparent activation energies ($\sim$1 kcal/mol) for the coil-to-helix transition.[36,37] The low barrier found here is qualitatively consistent with these results, but a quantitative comparison is complicated by the entropic contribution to the model barrier and the use of simple Arrhenius expressions which neglect viscosity effects[32] in the experimental data analysis.

Dynamical Properties

It is apparent from Figs. 3–5 that the mobility of the residues increases markedly at the end of the polypeptide chain. Residue 15 unwinds from the helix quite readily and exhibits rather large fluctuations after residues 14 and 15 have unwound. Residue 14 unwinds less readily and exhibits smaller fluctuations after unwinding. Residue 13 exhibits only occasional,

transient departures from the helix, even after the last two residues have unwound.

Since the helix–coil transition free-energy barriers are similar for all the residues, the reduced mobility of residues in the chain interior indicates that these residues have smaller effective diffusion constants. Unwinding of an interior residue requires simultaneous displacement of residues in the coil, so that larger frictional forces are involved.[38] The coil region does not move as a rigid body, however; the torsional motions are correlated so as to minimize dissipative effects. This is particularly apparent in the large displacements of Φ_{10} in Fig. 3. With Φ_{11} and Φ_{12} in extended conformations, the positive correlation of $\Delta\Phi_{10}$ and $\Delta\Phi_{11}$ tends to minimize the displacements of residues 14 and 15 when residue 13 moves, while the negative correlation of $\Delta\Phi_{10}$ and $\Delta\Phi_{12}$ also tends to minimize the displacement of residue 15 when residue 13 moves. Similar variations of mobility and torsional correlations have been observed in simulation studies of simple alkanes.[13–17]

The equilibrium constants s for adding residues to the helix are close to unity, so the rate constant k_r for removing a residue from the helix is equal to the rate constant k_f for helix growth (apart from corrections due to nonequilibrium effects[39]). Although the preliminary results obtained here are not sufficient to assign accurate values to these rate constants, their approximate magnitudes are $k_f \approx 10^9\ \text{sec}^{-1}$ for the last residue in a chain, $k_f \approx 10^8\ \text{sec}^{-1}$ for the next to the last residue, and $k_f < 10^8\ \text{sec}^{-1}$ for the internal residues. These rate constants have been approximated as reciprocals of the average time intervals between helix–coil transitions for residues at the helix–coil interface. The rate constants k_f would be expected to drop to a limiting value for residues further into the chain. Correlated torsional motions such as those described above will result in localized motions within the coil during unwinding, so that the rate will not depend on the overall size of the coil. A rough estimate based on these considerations suggests that the limiting rate constant for the model chain considered here is $k_f \approx 10^7\ \text{sec}^{-1}$. These values fall in the range of experimental results ($k_f \approx 10^7$–$10^{10}\ \text{sec}^{-1}$) obtained for a variety of polypeptides in different solvents.[37,40–42] In work which is presently in progress, the dynamics of the model described here is being examined over longer intervals of time. This work involves both direct diffusional simulations (for times >100 nsec) and simulations based on special techniques designed to yield more efficient sampling of the helix–coil transitions.[43] This work is expected to yield more detailed information on the role of correlated residue displacements in determining helix–coil rate constants, as well as accurate values for these rate constants. Studies of the equilibrium and dynamical properties of heteropolymers and interacting polypeptides are also underway.

We thank Professor Peter Wolynes for rewarding discussions. S.H.N. is a postdoctoral fellow under a grant provided by the Robert A. Welch Foundation. Other research support has been provided by the Research Corporation, the donors of the Petroleum Research Fund, administered by the American Chemical Society, and the National Science Foundation.

References

1. Engel, J. & Schwarz, G. (1970) *Angew. Chem., Int. Ed.* **9**, 389–400.
2. Schwarz, G. & Engel, J. (1972) *Angew. Chem., Int. Ed.* **11**, 568–575.
3. Teramoto, A. & Fujita, H. (1976) *J. Macromol. Sci., Rev. Macromol. Chem.* **15**, 165–278.
4. Némethy, G. & Scheraga, H. A. (1977) *Q. Rev. Biophys.* **10**, 239–352.
5. Creighton, T. E. (1978) *Prog. Biophys. Mol. Biol.* **33**, 231–297.
6. Lim, V. I. (1978) *FEBS Lett.* **89**, 10–14.
7. Rackovsky, S. & Scheraga, H. A. (1978) *Macromolecules* **11**, 1–8.
8. Karplus, M. & Weaver, D. L. (1976) *Nature* **260**, 404–406.
9. Sasaki, K., Dockerill, S., Adamiak, D. A., Tickle, I. J. & Blundell, T. (1975) *Nature* **257**, 751–757.
10. Boesch, C., Bundi, A., Oppliger, M. & Wüthrich, K. (1978) *Eur. J. Biochem.* **91**, 209+214.
11. McCammon, J. A., Gelin, B. R. & Karplus, M. (1977) *Nature* **267**, 585–590.
12. Flory, P. J. (1969) *Statistical Mechanics of Chain Molecules*, Wiley, New York.
13. Fixman, M. (1978) *J. Chem. Phys.* **69**, 1538–1545.
14. Helfand, E., Wasserman, Z. R. & Weber, T. A. (1979) *J. Chem. Phys.* **70**, 2016–2017.
15. Levy, R. M., Karplus, M. & McCammon, J. A. (1979) *Chem. Phys. Lett.* **65**, 4–11.
16. Evans, G. T. & Knauss, D. C. (1979) *J. Chem. Phys.* **71**, 2255–2262.
17. Pear, M. R. & Weiner, J. H. (1980) *J. Chem. Phys.* **72**, 3939–3947.
18. Richmond, T. J. & Richards, F. M. (1978) *J. Mol. Biol.* **119**, 537–555.
19. Levitt, M. & Warshel, A. (1975) *Nature* **253**, 694–698.
20. Levitt, M. (1976) *J. Mol. Biol.* **104**, 59+107.
21. Levitt, M. (1976) in *Models for Protein Dynamics*, CECAM Workshop Report, Université de Paris XI, Orsay, France.
22. Fixman, M. (1978) *J. Chem. Phys.* **69**, 1527–1537.
23. Pauling, L., Corey, R. B. & Branson, H. R. (1951) *Proc. Natl. Acad. Sci. USA* **37**, 205–211.
24. Lifson, S. & Oppenheim, I. (1960) *J. Chem. Phys.* **33**, 109–115.
25. Nozaki, Y. & Tanford, C. (1971) *J. Biol. Chem.* **246**, 2211–2217.
26. Weeks, J. D., Chandler, D. & Andersen, H. C. (1971) *J. Chem. Phys.* **54**, 5237–5246.
27. Pratt, L. R. & Chandler, D. (1977) *J. Chem. Phys.* **67**, 3683–3704.
28. Swaminathan, S. & Beveridge, D. L. (1979) *J. Am. Chem. Soc.* **101**, 5832–5833.
29. Pangali, C., Rao, M. & Berne, B. J. (1979) *J. Chem. Phys.* **71**, 2975–2981.
30. Alter, J. E., Andreatta, R. H., Taylor, G. T. & Scheraga, H. A. (1973) *Macromolecules* **6**, 564–570.
31. Ermak, D. L. & McCammon, J. A. (1978) *J. Chem. Phys.* **69**, 1352–1360.
32. Kramers, H. A. (1940) *Physica* **7**, 284–304.
33. Hermans, J. (1966) *J. Phys. Chem.* **70**, 510–515.
34. Rialdi, G. & Hermans, J. (1966) *J. Am. Chem. Soc.* **88**, 5719–5720.
35. Page, M. I. & Jencks, W. P. (1971) *Proc. Natl. Acad. Sci. USA* **68**, 1678–1683.
36. Tsuji, Y., Yasunaga, T., Sano, T. & Ushio, H. (1976) *J. Am. Chem. Soc.* **98**, 813–818.
37. Gruenewald, B., Nicola, C. U., Lustig, A., Schwarz, G. & Klump, H. (1979) *Biophys. Chem.* **9**, 137–147.
38. Jernigan, R. & Szu, S. C. (1976) *J. Polym. Sci., Polym. Symp.* **54**, 271–281.
39. Northrup, S. H. & Hynes, J. T. (1978) *J. Chem. Phys.* **69**, 5246–5260.
40. Zana, R. (1975) *Biopolymers* 14, 2425–2428.
41. Inoue, S., Sano, T., Yakabe, Y., Ushio, H. & Yasunaga, T. (1979) *Biopolymers* 18, 681–691.
42. Bosterling, B. & Engel, J. (1979) *Biophys. Chem.* **9**, 201–209.
43. Northrup, S. H. & McCammon, J. A. (1980) *J. Chem. Phys.* **72**, 4569–4578.

Received October 31, 1979
Accepted July 2, 1980